Design of JHF-MEBT with RF-Chopper

Shinian FU and Takao KATO*
China Institute of Atomic Energy (CIAE)
P. O. Box 275, Beijing 102413, China
*High Energy Accelerator Research Organization (KEK)
1-1 Oho, Tsukuba-shi, Ibaraki-ken, 305-0801, Japan

Abstract

The MEBT between the RFQ and DTL in JHF proton linac must accomplish two important tasks - beam matching and beam chopping, for the purpose of reducing beam losses in the intense-beam accelerator. RF-chopper is applied in the MEBT for its advantages in high deflecting field and compactness. The MEBT has been designed with eight quadrupoles, two bunchers and two RF-choppers, with a total length of 3m. The modified TRACE3-D code gives a beam edge separation of 4.3mm between the chopped and unchopped beams at a deflecting field of 1.6MV/m. An error study on the MEBT with multiparticle code is conducted. A coupled RF-chopper system is designed to reduce the demanded RF-power. It has been verified from HFSS simulations and cold-model measurements that the coupled system exhibits a fast transient time, almost the same as an independent cavity. An investigation on the unstable particles during transient time shows that the unstable particle ratio is as low as 0.08%, which satisfies our beam-loss control requirement.

1 Introduction

A 400-MeV linac is used as the injector of a 3-GeV fast-cycling ring in the JHF/JAERI joint project [1]. The linac provides a beam of 30 mA in peak current and 0.2 mA in average current and the current will become much higher in the upgrade plan. As an intense-beam linac, beam-loss control is a very essential requirement in the accelerator design for the reason that lost particles will induce strong radioactivity on the machine. It has been realized that beam matching is of great significance for minimizing the emittance growth and for avoiding beam halo formation, which is recognized as being one of the major causes for beam losses [2].

A 500-μsec macropulse from the ion source must be chopped into sub-pulses with a length of 278 nsec and a gap of 222 nsec for injection into the following ring. The chopped pulses should have a clear cut at the head and tail, because the unstable particles, which are insufficiently deflected during the transient time, may get into the following accelerators and then be lost.

The medium-energy beam-transport line (MEBT) between the 324-MHz RFQ and DTL has been designed to accomplish the two tasks: beam matching and chopping. Transverse and longitudinal matching can be achieved by means of quadrupoles and bunchers, respectively. RF deflector (RFD), as the chopper, is adopted in the MEBT owing to its advantages in high deflecting field and compactness. The two deflector cavities in the MEBT are coupled in order to reduce the total RF power demand. A short MEBT line is wanted for the conservation of the beam quality. The line must also leave sufficient spaces for installation of the beam diagnostics and elements connection. The RF power demanded by the RF choppers should be as less as possible.

In this report, the design detail is delineated. In the next section, an MEBT design using a modified TRACE3-D code is proposed. Section 3 discusses a mismatch in the MEBT caused by errors in the beam-line elements or the input beam parameters. The two RF-deflector cavities are designed to be a coupled system in the Section 4. The discussion about unstable particles in coupled RF-deflectors is conducted in Section 5.

2 MEBT Design

In order to trace the beam-deflection behavior, TRACE3-D has been modified so as to include a new element: RF deflector. The field distribution in the deflector cavity is calculated from MAFIA and directly read into TRACE3-D. In this way, the fringe E&H fields beside the deflecting electrode can be taken into account.

Table 1. Input beam parameters at the MEBT entrance.

Parameters	Type A	Type B
I (mA)	30	60
$\varepsilon^{x,y}_{RMS}$ (πmm-mrad)	0.187	0.375
ε^{z}_{RMS}(πMeV-Degree)	0.133	0.266

The output beam from the RFQ is assumed to have the parameters listed in Table 1. Type A stands for the 30-mA case and Type B for the 60-mA case for upgrading in the future. The MEBT design is proposed with a total length about 3 m (Fig. 1). In the beam-profile plot at the bottom of the figure, the beam centroid offset in the x-direction by the RF deflectors is depicted by the dark curve. The beam dump will be positioned at the element 18 for the chopped beam. The beam edge separation between the normal and deflected beams is 4.3mm at the beam dump. This separation is contributed from not only the two RF deflectors, but also the fourth quadrupole - element 16.

Beam-emittance growth for an unchopped beam has been studied by means of PARMILA simulations with 10,000

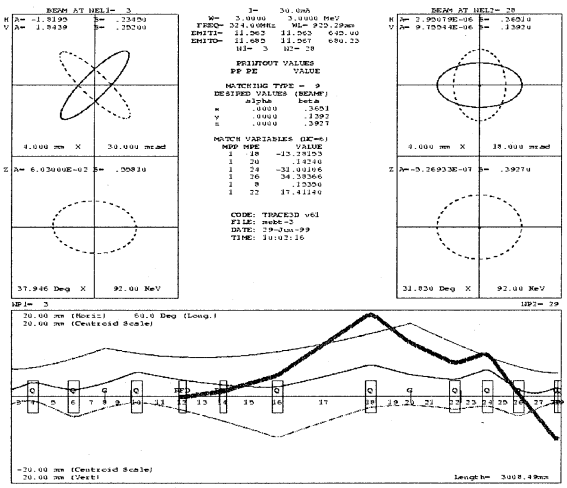

Figure 1. TRACE3-D output of the MEBT for an input beam of Type A with a current of 30 mA. The dark curve traces the beam centroid offset by the two RF deflectors.

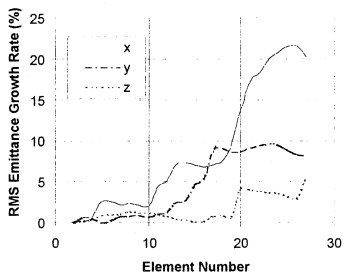

Figure 2. RMS emittance growth vs. the beam-line elements for a Type-A input beam.

particles. Figure 2 shows the RMS emittance variation versus the element of the beam line. The beam has RMS emittance growths of 20%, 8% and 5% in the x, y, z directions, respectively. In the MEBT, a sufficient space is available for beam diagnostics, mechanical installation and the connection of the transport elements. It is necessary to measure the beam emittance during long-term operation. To do this, the drift space of element 17 is long enough for installing a bending magnet, which leads the beam to a diagnostics beam line.

3 Study on Errors in the MEBT

To understand the importance of beam matching in the MEBT, error simulations of the MEBT were conducted which cover the element error and input beam error based on the reference design in the last section. We present the effect of errors on the output beam of the MEBT in term of a mismatch factor and multiparticle simulations of the mismatched beam in the following DTL by the LINSAC code [3]. Concerning the misalignment error, some steering magnets are suggested in the reference design.

When the matched beam line is used, we see no obvious beam halos in the DTL. The rms emittance growth in the DTL is also small; for instance, the longitudinal emittance growth is 1.14 times. If 99.9% particles are considered, it becomes 1.78 times. However, if the elements in the MEBT have errors or the input beam into the MEBT has different Twiss parameters, the beam into the DTL becomes mismatched. Mismatch factor is defined as:

$$MMF = \left[\frac{1}{2}\left(R+\sqrt{R^2-4}\right)\right]^{1/2} - 1 \qquad (1)$$

with $R=\beta\gamma'+\gamma\beta'-2\alpha\alpha'$; here, Twiss parameters with a prime stand for a mismatched beam with the same phase ellipse area as a matched beam. To show the effect of an element error, we assume, for instance, that the gradient of the first quadrupole varies by 2.6%. The resultant mismatching factors are MMF_x=20%, MMF_y=24% and MMF_z=2% in the x, y and z directions, respectively. If the input beam into the MEBT has a 10% error in the Twiss parameter β_z, it induces an MMFz of 5%. The same amount error in β_x results in both MMF_x=19% and MMF_y=25%, but 2.5% in MMF_z. This means that the variations of the emittance shapes in the two transverse directions are coupled with each other by a space-charge effect in the MEBT.

In the longitudinal direction, a voltage error of 2.5% in the second buncher can result in an MMF_z of 9.5% at the entrance of the DTL. Consequently, a nonlinear tail is generated in the phase-space plot (Fig. 3), which results in an rms emittance growth of 1.18 times, and an emittance growth of 4.14 times if 99.9% of the particles are included.

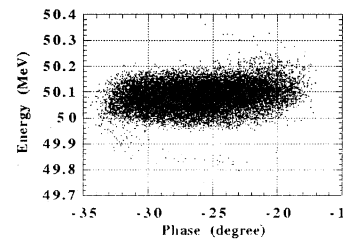

Figure 3. Longitudinal emittance of the mismatched beam at the exit of the DTL when MMF_z is 9.5% at the entrance.

To offset the misalignment error in the output beam from the RFQ, some steering magnets are required to be installed in the MEBT for two purposes: 1) beam alignment in the following DTL; 2) beam-loss control in the narrow gap of the RF-deflectors. Three steering magnets should be inserted into the MEBT at the locations of the end of the RFQ, after RFD2 and Q6, respectively. The resulted allowance to the initial beam error thus becomes large ($dx<\pm0.5$ mm, $dx'<5$ mrad; $dy<\pm0.2$ mm, $dy'<3$ mrad), if the maximum available steering field of the magnet is about $B\times L<1300$ Gauss-cm.

4 Coupled Chopper System

A 324-MHz RF deflector cavity has been designed using MAFIA and HFSS codes and a cold model cavity was measured with a satisfactory result of a loaded Q less than 10[4] for the purpose of fast rise/fall times. It is reached by means of a pair of large coupling loops inserted into the cavity. As a result, most of the input RF power to the cavity goes out from the cavity to a matched load. To halve the RF-power demanded for the two RF-choppers, we designed the two RF-deflectors to be coupled with a coaxial line. It is

expected three modes (0, $\pi/2$ and π) will appear. With a coaxial cavity of $\lambda/2$ in electric length, an HFSS simulation shows three modes in Fig.4. It is found from the figure that the $\pi/2$ mode oscillates at frequency of 324 MHz and the –3dB bandwidth is 34 MHz. This means that the coupled system behaves in almost the same way as an independent cavity when operated in the $\pi/2$ mode. The phase relation between the two cavities was investigated by observing the oscillation of the deflecting field in the two cavities with the post-processor of HFSS code. It is found that the $\pi/2$ mode has a phase shift of π between the two RF-deflector cavities.

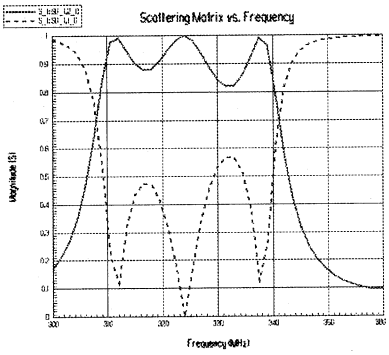

Figure 4. Scattering parameters S_{21}(solid) and S_{11}(dashed) vs. frequency from HFSS simulation of a coupled RF-deflector system of 324 MHz. It shows three modes with a bandwidth of 34 MHz.

A measurement was conducted with two 434 MHz RF-deflector cavities. When they were connected by a coaxial line with an electric length of $N\lambda$, with N being an integer, the S_{21} spectrum (Fig.5) from a network analyzer displayed the same feature as in an HFSS simulation. It exhibits three modes and the $\pi/2$ mode oscillates at 434.75 MHz. The bandwidth is 32.7 MHz, almost the same as the bandwidth of an independent cavity, which is 34.3 MHz.

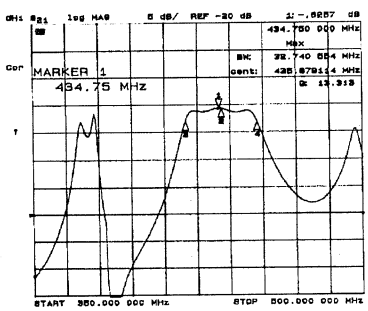

Figure 5. S_{21} spectrum of a coupled-deflector system of 434 MHz from measurement with a network analyzer. The bandwidth of 32.7 MHz is almost the same as that of a single cavity.

5 Analysis on Unstable Particles

To investigate the unstable particle behavior during transient time, some PARMILA simulations of the MEBT were conducted with a particle scraper having a width of 19 mm in the x direction. Figure 6 shows that the unstopped particle ratio in a bunch declines as the deflecting field increases toward its full value of 1.6 MV/m. The bunch meeting the field of 40%, 65% and 85% will contribute to the unstable particles. They can be further reduced by the three scrapers between DTL tanks, as indicated by the circles in the figure. The resultant unstable particle ratio at the exit of the DTL becomes less than 0.08%, which is a satisfactory low value for our beam loss control.

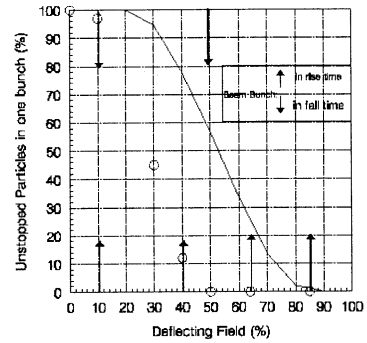

Figure 6. Unstopped particles ratio in one bunch vs. the deflecting field variation from PARMILA simulations. The arrows stand for the bunch distribution and the circles for the case with scrapers between the three DTL tanks.

Above result comes from the assumption that the two RF deflectors have the same field during the transient time. However, when they are coupled with a coaxial line, there is a time delay between the two. According to the results in the last section, the coaxial line length should be $N\lambda/2$, and the distance between the two RF-deflectors should be $M\beta\lambda/2$, with N and M being odd or even integer simultaneously, in order to keep the beam bunches synchronized with the RF field in the two deflectors. When the two integers are not equal, the beam bunches meet a different field during the transient time in the two deflectors. We choose M equal to 6 and N equal to 2, and the resulted field a bunch meet is analyzed in Table 2. Only the three bunches meeting with average fields of 38%, 63% and 83% will contribute unstable particles, almost the same as in Fig 6. So the coupled deflector system does not introduce additional unstable particles.

Table 2 Deflecting field in the two cavities and their effect.

Field in Cavity 1	Field in Cavity 2	Total Field	Average Field
0	10%	10%	5%
0	40%	40%	20%
10%	65%	75%	**38%**
40%	85%	125%	**63%**
65%	100%	165%	**83%**
85%	100%	185%	93%

References

[1] T. Kato, KEK Report 96-17, Feb. 1997.
[2] Y. Yamazaki, Proc. of 1996 Inter. Linac Conf., 26-30, Aug. 1996, Geneva, Switzerland.
[3] T. Kato, Proc. of 1994 Inter. Linac Conf., Tsukuba, Japan, p.523.
[4] S. Fu, T. Kato, F. Naito and K. Yoshino, Proc. of LINAC'98, Chicago, USA, Aug. 23-28,1998, p. 585